Bled Workshops
in Physics
Vol. 13, No. 1
p. 23

Proceedings of the Mini-Workshop
Hadronic Resonances
Bled, Slovenia, July 1 - 8, 2012

Resonances in photo-induced reactions

M. Ostrick

Institut für Kernphysik, Johannes-Gutenberg-Universität Mainz, J.-J.-Becher-Weg 45, 55128 Mainz, Germany

Abstract. The extraction of baryon resonance parameters from experimental data and their interpretation within QCD are central issues in hadron physics. To achieve these goals it is an essential prerequisite to have a sufficient amount of precision data which allows an unambiguous reconstruction of partial wave amplitudes for different reactions. Over the last years an intense effort has started to study photon-induced meson production. Many single and double spin-observables have been measured for the first time. This experimental progress will be illustrated by means of single and double π^0 photo-production. The focus will be on the impact of the new data for the unambiguous reconstruction of partial wave amplitudes.

1 Introduction

Meson scattering and meson production reactions below 3 GeV distinctively exhibit resonances, clearly organized in terms of flavor content, spin and parity, sitting on top of a non resonant "background. In lack of stringent predictions from strong QCD these resonances are usually interpreted in constituent quark models as excitations of massive quasi-particles bound by a confining potential. However, also the strong meson-baryon and meson-meson interaction could give rise to dynamically generated resonances. Chiral unitary methods and coupled channel calculations provide a theoretical framework to study the importance of resonances without including them explicitly in a model. Furthermore, lattice QCD simulations started to become predictive for dynamical quantities like strong decay widths of resonances and scattering phase shifts [1]. In the past, only calculations of approximate mass spectra in the heavy pion limit, where excited baryons are stable particles, were possible.

Empirically, N^* and Δ^* baryon resonance parameters like mass, width or pole position have been extracted for many years by partial-wave analyses of elastic and charge-exchange pion-nucleon scattering experiments. The most recent analysis of existing πN data has been performed by the George Washington Group [2]. Today there is no running experiment dedicated to study πN scattering anymore. However, options for a new generation of experiments with pion beams at Hades/GSI [3], ITEP [4] and J-PARC [5] are presently under discussion.

Instead of πN scattering, an immense effort started during the last decade to study baryon resonances with electromagnetic probes at various laboratories,

mainly ELSA, Graal, JLAB, LEPS, LNS and MAMI. The motivation for this ongoing effort is 2-fold. The initial idea was to substantiate or to disprove the existence of questionable resonances or even to discover new states that couple only weakly to πN. Especially, above 2 GeV an abundance of states is predicted by quark models which are not identified in πN partial wave analyses. This fact is often called the "missing resonance" problem. As historically all information about resonances came from pionic reaction, the hope was to discover new states in e.g. KΛ, KΣ, ηN or ωN final states. The PDG lists in their latest edition a couple of new states which have been seen in some analyses of recent data [6]. However, there are still many ambiguities and the discussion is ongoing.

The second objective are high precision measurements of the excitation of established resonances with real and virtual photons in order to relax the model constraints in the analyses and understand the influence of background on the extraction and interpretation of resonance properties. Single and double spin observables turned out to be an indispensable prerequisite to address both issues. Such measurements with sufficient acceptance and statistics became technically feasibly only recently. A brief overview of the facilities is given in section 2.

A completely different approaches to baryon spectroscopy are presently being developed at the BES-III e^+e^- collider , where decays like $J/\psi \rightarrow \bar{N}N^* \rightarrow \bar{N}N\pi$ have been observed, or at the COMPASS experiment at CERN, where diffractive processes like $pp \rightarrow pp\pi\pi$ clearly show resonant structures. One important milestone in future experimental baryon spectroscopy will be the combination of all empirical information from very different experiments in order to identify universal, i.e. process independent, properties of genuine nucleon excitations and to quantify the impact of coupled channel dynamics.

2 Photon beam facilities

During the last ten years we noticed an enormous increase in high precision measurements of many single and double spin observables in photo-induced meson production. The experiments are still ongoing and many results are still preliminary. The reason for this unprecedented development was the combination of high-intensity polarized beams, polarized targets and hermetic detector systems which was technically realized at the CLAS spectrometer in Hall B at Jefferson Lab [7], the Crystal-Barrel experiment at the ELSA stretcher ring [8] and the Crystal Ball experiment at the Mainz Microtron MAMI [9]. CLAS is a large acceptance spectrometer based on a toroidal magnetic field configuration. Tracking chambers and time-of-flight detectors provide charge particle identification and momentum resolution. At CLAS, energy tagged, polarized photon beams with up to 6 GeV can be used. The Crystal Barrel calorimeter consisting of 1230 CsI(Tl) crystals is the core of the experimental setup at ELSA and provides excellent acceptance and resolution for multi-photon final states. The Crystal Ball at MAMI (see Fig. 2) consists of 672 NaI(Tl) crystals covering 93% of the full solid angle with an energy resolution of 1.7% for electromagnetic showers at 1 GeV. For charged particle tracking and identification two layers of coaxial multi-wire proportional

chambers and a barrel of 24 scintillation counters surrounding the target are installed. The forward angular range is covered by the TAPS calorimeter consisting of BaF2 detectors and a Cerenkov detector.

The polarized target technique at all labs is based on Dynamic Nucleon Polarization (DNP) of solid-state target materials such as butanol, deuterated butanol, NH_3 or ^6LiD. The material is spin polarized by microwave pumping in an external magnetic field of 2.5T at temperatures of about 100mK. During the measurements, the spin orientation is frozen at temperatures of down to 20mK by a moderate longitudinal or transverse magnetic holding field of about 0.5T. The main technical challenge was the construction of a horizontal cryostat that fits into the detector geometry and keeps a temperature of about 20mK without adding too much material that would limit the particle detection. The underlying concept of the targets presently used at ELSA, JLAB and MAMI was developed in Bonn [10] and was successfully used for the first time in 1998 for measurements of the GDH sum rule in Mainz [11].

Fig. 1. Crystal-Ball detector at MAMI and the horizontal cryostat of the frozen spin target, which keeps temperatures of about 20mK.

3 $\gamma N \rightarrow \pi N$

The photo-production of pseudoscalar mesons has four spin degrees of freedom which define four complex scattering amplitudes for each isospin. These amplitudes manifest themselves in 16 different single and double spin observables, including experiments with polarized target, beam and nucleon recoil polarimetry. It is well known for a long time that the full knowledge of 8 selected observables at each energy and scattering angle completely determines all amplitudes in a mathematical sense. Such a procedure is called a "Complete Experiment" [12]. It would then allow us to predict all remaining observables. However, in a real situation with statistical and systematic uncertainties this procedure is much more difficult. Furthermore, the goal is not a "Complete Experiment" and the reconstruction of the 4 helicity amplitudes but an understanding of the underlying dynamics. For this, the knowledge of all relevant partial wave or multipole amplitudes is much more important.

Up to a certain maximum orbital angular momentum l_{max}, all $4l_{max}$ complex multipole amplitudes have to be determined from experiment (see Table 1). It can be shown that even a "Complete Experiment" is only of limited value to reach this goal because of the freedom to choose an angular and energy dependent overall phase [13]. Therefore, one has to determine the relevant multipoles directly from experimental data. Each observable, $O_i(W,\theta)$, can be expanded in term on Legendre polynomials:

$$O_i(W,\theta) = \sin^{\alpha_i}\theta \sum_{k=0}^{k_{max}} a_{ik}(W) P_k(\cos(\theta)), \quad \alpha_i = \{0,1,2\}. \tag{1}$$

Here k_{max} is given by the truncation to a certain maximum angular momentum. The coefficients $a_{ik}(W)$ are bilinear combinations of the $4l_{max}$ complex multipole amplitudes which can be reconstructed from the coefficients. For a detailed discussion of the concepts of a "Complete Experiment" and such a truncated partial wave analysis see [13].

Table 1. Multipole decomposition of the pion photo-production amplitude for $l_\pi \leq l_{max} = 2$. For each isospin, $4l_{max}$ complex multipoles have to be determined from experiment.

l_π	0	1			2			
J^p	$\frac{1}{2}^-$	$\frac{1}{2}^+$	$\frac{3}{2}^+$		$\frac{3}{2}^-$		$\frac{5}{2}^-$	
multiplole	E_{0+}	M_{1-}	M_{1+}	E_{1+}	M_{2-}	E_{2-}	M_{2+}	E_{2+}

A direct reconstruction of the relevant partial wave amplitudes was achieved for the first time in the energy region of the $\Delta(1232)$ resonance using a truncation to s- and p-waves ($l_{max} < 2$) and additional theoretical constraints [14].

At higher enegies this procedure requires precision measurements of several spin observables with a sufficiently fine energy binning, e.g. 10 MeV, and a full angular coverage. Below $E_{CM} \sim 2$ GeV, where a truncation to F- or G-wave ($l_{max} < 3$ or 4) is possible, already the measurement of 4-6 spin and double-spin observables could provide sufficient constraints for such a direct reconstruction. This has been shown in [15] using generated pseudo-data with realistic uncertainties that will be achieved with the Crystal-Ball experiment at MAMI within the next years. Preliminary results for many new target and beam-target asymmetries from ELSA, JLAB and MAMI have been presented e.g. at the last NSTAR conference [16]. However, the direct reconstruction of multiploles has not yet been achived above the $\Delta(1232)$ resonance region and one has to rely on fits using models for the energy-dependent amplitudes. Figure 3 summarizes the current status of such model dependent analyses in the case of the important lowest order multipole amplitudes, $J^p = 1/2^+(M_{1-})$ and $J^p = 1/2^-(E_{0+})$. Even at relatively low energies in the second resonance region there are significant deviations between different models. A summary of our current knowledge of multipole amplitudes for different flavor states can be found in [21].

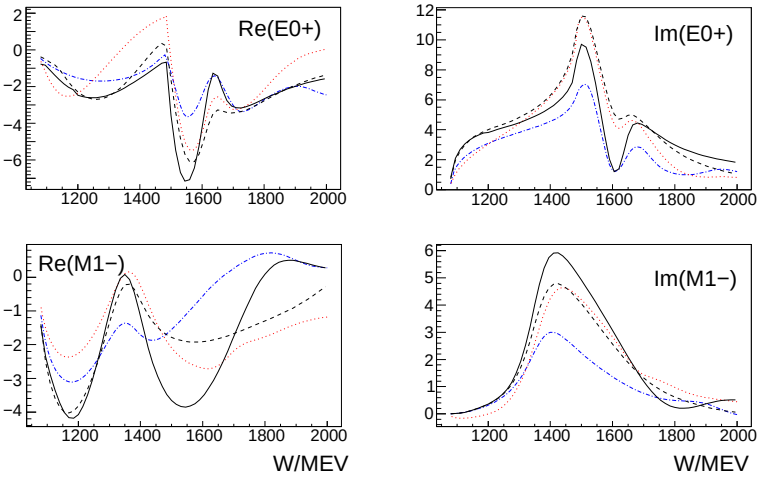

Fig. 2. Lowest order multipole amplitudes of the $\gamma p \to \pi^0 p$ reaction in units of $10^{-3}/M_\pi$. The curves are derived from fits of different models to existing data. The black solid and dashed lines represent the SAID 2011 and the SAID Chew-Mandelstam fits [17, 18], the MAID analysis gives the red dotted line [19]. Finally, the blue dashed-dotted curve is derived from the Bonn-Gatchina analysis [20].

In the case of the $\gamma p \to \pi^0 p$ reaction close to threshold a direct reconstruction of the amplitudes is more simple as the dynamics is dominated only by one s-wave, E_{0+} and 3 p-waves, M_{1-}, M_{1+} and E_{1+}. Furthermore, these multipoles are real between the $\pi^0 p$ and $\pi^+ n$ production thresholds. Above the $\pi^+ n$ threshold the E_{0+} amplitude becomes complex and shows a strong energy dependence due to the unitary cusp [22]. The imaginary parts of the p-waves remain negligible below $\sim$ 180 MeV. With this truncation, the real parts of the multipoles can be reconstructed from measurements of two observables only, namely the differential cross section and the photon beam asymmetry

$$\Sigma = \frac{\sigma_\perp - \sigma_{||}}{\sigma_\perp + \sigma_{||}}. \tag{2}$$

Here $\sigma_\perp$ and $\sigma_{||}$ denote the differential cross sections with the photon polarization vector perpendicular and parallel to the $p\pi^0$ reaction plane. Both observables have recently been measured from threshold up to the Δ resonance region with unprecedented accuracy at the Crystal-Ball experiment at MAMI [23]. Fig. 3 show as an example the results of these measurements at the CM angle of 90° as function of the incoming photon energy. The new data are compared to existing data and ChPT calculations with updated low-energy parameters [25] as well as the 2001 version of the DMT dynamical model [26]. The reconstruction of the multipoles is almost final and will be published soon [24].

With all relevant multipoles fixed by experiment the additional measurement of target (T) and beam-target (F) spin asymmetries will provide sensitivity to the charge exchange $\pi^+ n \to \pi^0 p$ scattering length from the unitary cusp which enters directly in the imaginary part of the E_{0+} amplitude. Therefore, threshold

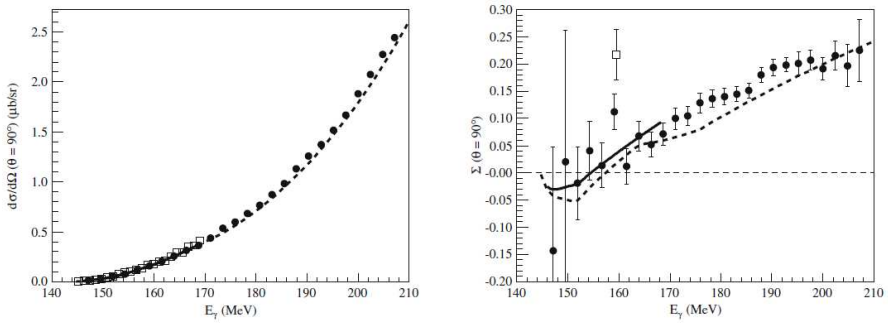

Fig. 3. Preliminary results from Crystal Ball at MAMI (solid circles) of the differential cross section and photon asymmetry for the $\gamma p \to \pi^o p$ reaction at pion CM angle of 90° compared to the older data from MAMI ([22], open squares) as well as some theory calculations. The solid lines are preliminary ChPT fits to the new data [25] and the dashed lines are a dynamical model [26].

π^0photo-production will enable us to study strong and electromagnetic isospin breaking in πN scattering by comparing the charge exchange scattering lengths for $\pi^+ n \to \pi^0 p$ and $\pi^- p \to \pi^0 n$ [23]. The ladder has recently been measured in pionic hydrogen [27].

4 $\gamma N \to \pi\pi N$

When looking at the production of meson pairs like $\pi\pi$ of $\pi\eta$ it is obvious that the dynamics can be much more complex and an analysis will be even more model dependent than in the case of single meson photo-production. Nevertheless, $\pi\pi N$ and $\pi\eta N$ finals states have attracted a lot of interest during the last years. These processes allow us to study resonances which have no significant branching ratio for a direct decay into the nucleon ground state. This is possible via sequential decays which involve intermediate excited states like $R \to R'\pi \to N\pi\pi$. Here R and R' denote nucleon resonances. Such decay chains are a phenomenon that can be observed in other quantum systems like atoms or nuclei as well. The theoretical interpretation is usually based on isobar models or effective field theories [28–32]. Typically, the reaction amplitude is constructed as a sum of background and resonance contributions. The background part contains nucleon Born terms as well as meson exchange in the t channel. The resonance part is a coherent sum of s-channel resonances decaying into $\pi\pi N$ via intermediate formation of meson-nucleon and meson-meson states ("isobars"). Despite significant differences between the models, all of them provide an acceptable description of the existing data. This observation clearly demonstrates, that further experimental and theory studies are necessary.

With the Crystal-Ball at MAMI we have recently studied the $\gamma N \to \pi^0\pi^0 N$ reactions by measurements of cross sections [33] and beam helicity asymmetries [34, 35].

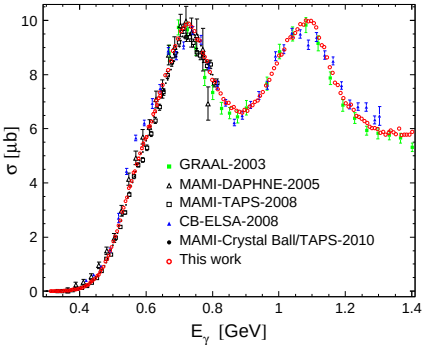

Fig. 4. Total cross section for the $\gamma p \rightarrow \pi^0\pi^0 p$ reaction as function of the incoming photon energy. The open circles show the precision that has been obtained at MAMI. Further information and references can be found in [33].

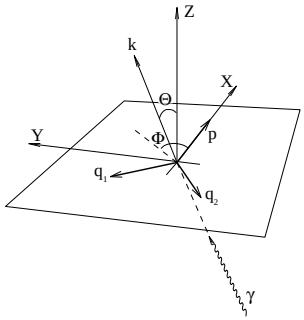

Fig. 5. The coordinate system is fixed by the momenta of the incident-photon, $\mathbf{k}$, out-going proton, $\mathbf{p}$ and the two pions, $\mathbf{q}_1$, and $\mathbf{q}_2$, in the center of mass system.

Fig. 4 shows the existing data for the total cross section. It is widely accepted that the $D_{13}(1520)$ resonance decaying to $\pi\Delta$ channel is responsible for the first peak at $E_\gamma \approx 730$ MeV. However, the underlying dynamics down to threshold as well as the behavior at higher energies have not been well understood so far. E.g., the minimum at $W = 1.6$ GeV and the second maximum at $W = 1.7$ GeV are described in Ref. [32] by the destructive interference between D_{13} and D_{33} partial wave amplitudes. In other models this behavior is explained by different resonance contributions, e.g. in the F_{15} partial wave. The high accuracy of the MAMI new data allowed us to make first steps towards a model independent partial wave analysis for the first time. In case of meson pair production the helicity amplitudes depend on the incoming photon energy, E_γ, the meson energies, ω_1 and ω_2 (Dalitz-Plot) and two angles, Θ and Φ, which are explained in Fig. 5. The angular distributions normalized to the total cross section, $W(E_\gamma, \omega_1, \omega_2, \Theta, \Phi) = \frac{1}{\sigma} \cdot \frac{d\sigma}{d\Omega}$ can now be expanded in terms of spherical harmonics $Y_{LM}(\Theta, \Phi)$. In a first step, we average the distributions over the meson energies, ω_1, ω_2:

$$W(E_\gamma, \Theta, \Phi) \equiv \frac{1}{\sigma} \int d\omega_1 d\omega_2 \frac{d\sigma}{d\Omega} = \sum_{L \geq 0} \sum_{M=-L}^{L} \sqrt{\frac{2J+1}{4\pi}} W_{LM}(E_\gamma) \cdot Y_{LM}(\Theta, \Phi) \tag{3}$$

This expansion determines the general structure of an angular distribution analogous to the expansion of the cross section for single-meson photo-production in terms of the Legendre polynomials (see Eq. 1). The moments $W_{LM}(E_\gamma)$ are bilinear combinations of the partial wave amplitudes. The exact relations have been worked out explicitly by Fix and Arenhoevel in ref. [36]. With the high precision data from MAMI it was possible to determine the moments $W_{LM}(E_\gamma)$ for the first time. The results are shown in Fig. 6. In case of the production of two

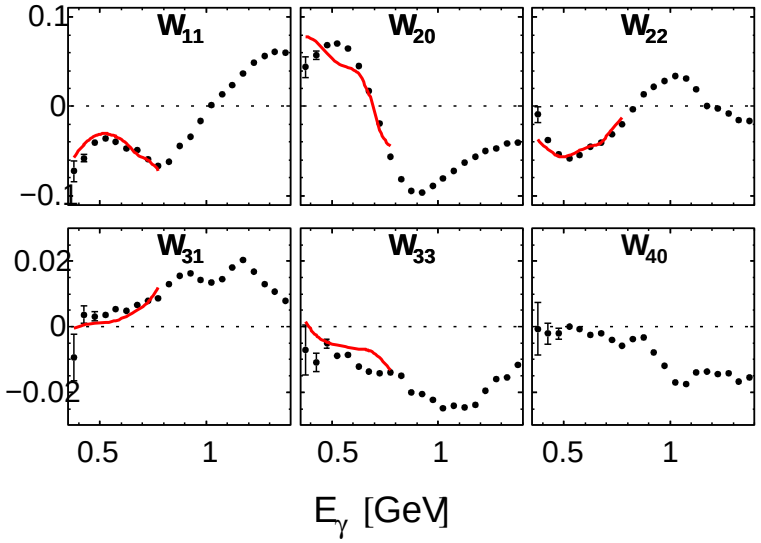

Fig. 6. First moments W_{LM} (normalized such that $W_{00} = 1$) as a function of the incident-photon energy. Our experimental results are shown by filled circles. The solid lines show the results of an isobar model fit [37].

identical particles, e.g. $\gamma p \rightarrow \pi^0\pi^0 p$, it can be shown, that the imaginary parts vanish exactly ($\mathrm{Im}(W_{LM}) = 0$). Already at low energies, the quantities W_{20} and W_{22}, which are given by an incoherent sum $J^P = 3/2^-$ and $3/2^+$ partial wave amplitudes, achieve relatively large values. This observation indicates an additional strong $3/2^-$ contribution, interfering with the $D_{13}(1520)$ resonance. This could support the dynamics found in Ref. [32] where a strong contribution from the $D_{33}(1700)$ resonance was found. Of course, the analysis of the moments $W_{LM}(E_\gamma)$ is only a very first step towards a full partial wave analysis of meson pair production processes. Nevertheless, it shows that data with very high precision, which will be available also for other observables in the future, will allow us to reduce the model dependence in the analysis procedures even for more complex final states significantly.

5 Conclusion

During the last decade an immense effort started to study baryon resonances in photo-induced meson production at various laboratories, mainly ELSA, Graal, JLAB, LEPS, LNS and MAMI. New high precision data for many spin observables are expected in the near future. A prerequisite for an unambiguous, model-independent extraction of resonance parameters is the reconstruction of partial wave or multipole amplitudes from experimental data. Resonances as well as effects from coupled channel dynamics manifest themselves in the analytic properties of these amplitudes. The upcoming data will allow us to minimze the model dependence in the determination of partial wave amplitudes in a systematic way.

This goal has already been achieved in π^0 photo-production close to threshold. The methods will be extended to higher photon energies and other final states (ηN, KΛ, $\pi\pi$N, etc.).

References

1. S. Prelovsek, C. B. Lang, and D. Mohler, Bled Workshops in Physics **12**, 73 (2011).
2. R. Arndt et al., Physical Review C **74**, 045205 (2006).
3. Symposium on baryon resonance production and electromagnetic decays, www.hades2012.pl
4. I. I. Alekseev, arXiv:1204.6433v1 (2012).
5. H. Fujioka, Hadron nd Nuclear Physics **9** , 150 (2010).
6. J. Beringer et al. (Particle Data Group), Phys. Rev. D**86**, 010001 (2012)
7. B. Mecking et al., Nucl. Instr. and Meth. A **503**, 513 (2003).
8. D. Elsner, Int. J. of Mod. Phys. E **19**, 869 (2010).
9. A. Thomas, Eur. Phys. J. Special Topics **198**, 171 (2011).
10. C. Bradtke et al., Nucl. Inst. and Meth. A **436**, 430 (1999).
11. J. Ahrens et al., Phys. Rev. Lett. **97**, 1 (2006).
12. I. Barker, A. Donnachie, and J. Storrow, Nucl. Phys. B **95**, 347 (1975).
13. L. Tiator, AIP Conf. Proc. **162**, 162 (2012) and contribution to this workshop.
14. R. Beck et al., Phys. Rev. C **61**, 1 (2000).
15. R. L. Workman et al., Eur. Phys. J. A **47**, 143 (2011).
16. V.Burkert, M.Jones, M.Pennington, D.Richards (ed.) AIP Conf. Proc. **1432**, 1 (2012).
17. R. L. Workman, W. J. Briscoe, M. W. Paris, and I. I. Strakovsky, Phys. Rev. C **85**, 025201 (2012).
18. R. Workman et al., Phys. Rev. C **86**, 1 (2012).
19. D. Drechsel, S. S. Kamalov, and L. Tiator, Eur. Phys. J. A **34**, 69 (2007).
20. A. V. Anisovich et al., Eur. Phys. J. A **48**, 15 (2012).
21. A. V. Anisovich et al., Eur. Phys. J. A **48**, 88 (2012).
22. A. Schmidt et al., Phys. Rev. Lett. **87**, 1 (2001).
23. D. Hornidge and a. M. Bernstein, Eur. Phys. J. Special Topics **198**, 133 (2011).
24. D. Hornidge et al., submitted to Phys. Rev. Lett. (2012).
25. C. Fernández-Ramírez et al., Phys. Lett. B **679**, 41 (2009).
26. S. Kamalov et al., Phys. Rev. C **64**, 1 (2001).
27. D. Gotta et al., AIP Conference Proceedings **1037**, 162 (2008).
28. J. Gómez Tejedor and E. Oset, Nucl. Phys. A **600**, 413 (1996).
29. M. Ripani et al., Nucl. Phys. A **672**, 220 (2000).
30. A. Fix and H. Arenhövel, Eur. Phys. J. A **135**, 115 (2005).
31. H. Kamano, B. Juliá-Díaz, T. S. H. Lee, a. Matsuyama, and T. Sato, Phys. Rev. C **80** (2009).
32. U. Thoma et al., Phys. Lett. B **659**, 87 (2008).
33. V. Kashevarov et al., Phys. Rev. C **85**, 1 (2012).
34. F. Zehr et al., Eur. Phys. J. A **48**, 1 (2012).
35. M. Oberle et al., submitted to Eur. Phys. J. A (2012).
36. A. Fix and H. Arenhövel, Phys. Rev. C **85**, 035502 (2012)
37. V. L. Kashevarov et al., Phys. Rev. C **85**, 1 (2012).